

## Lattice-dynamical evaluation of thermodynamic properties and atomic displacement parameters for beryl using a transferable empirical force field

TULLIO PILATI,<sup>1</sup> FRANCESCO DEMARTIN,<sup>2</sup> AND CARLO MARIA GRAMACCIOLI<sup>3</sup>

<sup>1</sup> CNR, Centro per lo Studio delle Relazioni tra Struttura e Reattività Chimica, Via Golgi 19, I-20133 Milano, Italy

<sup>2</sup> Dipartimento di Chimica Strutturale e Stereochimica Inorganica, Università degli Studi, Via Venezian 21, I-20133 Milano, Italy

<sup>3</sup> Dipartimento di Scienze della Terra, Sezione Mineralogia, Università degli Studi, Via Botticelli 23, I-20133 Milano, Italy

### ABSTRACT

Using empirical potentials derived from fitting the vibrational frequencies of a group of silicates and oxides, and crystallographic information, a Born-von Karman rigid-ion lattice-dynamical model has been applied to the whole Brillouin zone in beryl. The Raman and infrared spectra are satisfactorily reproduced and interpreted by these calculations; there is also very good agreement with atomic displacement parameters derived from accurate crystal-structure refinement by various authors and with experimental values of thermodynamic functions for the anhydrous phase at different temperatures. The agreement of our calculations with experimental data of independent origin and nature demonstrates the potential of such a procedure.

### INTRODUCTION

Following our interest in the field, which started from molecular crystals (e.g., Gramaccioli 1987 and references therein), we have tried to extend our harmonic lattice-dynamical calculations to minerals (Pilati et al. 1990, 1993a, 1993b, 1994, 1995, 1996a, 1996b, 1997). For such purposes, the Born-von Karman procedure has been adopted, using a rigid-ion model extended to the whole Brillouin zone.

The initial scope of our calculations was concerned with theoretical evaluation of atomic displacement parameters (ADP) and their comparison with corresponding results obtained from crystal-structure refinement. Then we began interpreting vibrational spectroscopy data, such as Raman and infrared spectra, and especially estimating the values of thermodynamic functions.

The first systematic attempt to derive thermodynamic properties for a whole series of different minerals from spectral data, using statistical-mechanical procedures, is that of Kieffer (1979a, 1979b, 1979c, 1980, 1982). However, a Born-von Karman lattice-dynamical model is more accurate; no fit is needed for several experimental data specific for a single phase, and there is an immediate connection with force fields. The possibility of wide application of Born-von Karman lattice-dynamical models to minerals, using empirical valence force-field (VFF) parameters is supported by several authors who also used the rigid-ion model, such as Rao et al. (1988), Dove et al. (1992), Kihara 1993, and Ghose et al. (1994). An important advantage of such lattice-dynamical models is that spectroscopic information is helpful for deriving these empirical force-field parameters only, on a best-fit basis to experimental values; if the force fields are transferable, such information may not even be essential for each par-

ticular compound (e.g., Pilati et al. 1996a, 1996b). The need to know all possible information concerning the vibrational frequencies for each particular compound could be a serious drawback, because, apart from the problem of selecting the fundamentals, many of these frequencies are often missing in the experimental measurements of Raman or infrared spectra, either because their intensity is too weak or because they are not active due to symmetry. A significant example occurs for garnets; because of symmetry, more than 50% of the modes at the origin of the Brillouin zone are both Raman and IR inactive.

Successful applications of Born-von Karman lattice dynamics to minerals using more elaborate schemes, such as shell models or the quasi-harmonic approximation, are due to several authors such as Price et al. (1987a, 1987b), Winkler et al. (1991), and Patel et al. (1991). In most of these works, good agreement was achieved with the experimental values of some thermodynamic functions such as the specific heat and entropy at different temperatures, and the possibility of using transferable empirical force fields for such purposes has been confirmed also. However, the inadequacy of the rigid-ion model with respect to these more advanced models is generally evident for the highest frequencies only. In most cases, the lowest vibrational energy levels are reproduced with comparable accuracy, and the contribution of these low levels is usually the overwhelming one in accounting for thermodynamic functions and ADP. Rigid-ion models similar to ours were used recently and successfully by several authors, such as Dove et al. (1992) and Catti et al. (1993) to derive physical properties of calcite and aragonite, and Keskar and Chelikowsky (1995) to calculate thermodynamic properties of silica polymorphs.

Unfortunately, for minerals in general there are very

few determinations of the acoustic branches of the phonon dispersion curves, which are the most important for calibrating the potentials used in our lattice-dynamical calculations. At present, the great majority of experimental data available for these purposes consists of Raman and infrared spectra. In this respect, a fundamental inconvenience is that measurements on single crystals are relatively scarce, and there are still insufficient (and often inaccurate) data, particularly concerning the lowest frequencies, which, as we have seen, are indeed the most important for our purposes. Therefore, one might wonder whether a notable part of the disagreement between theoretical and experimental values, more than the model, might instead be caused by lack of adequate experimental data. Consequently, there is the interesting possibility that at the present state of the art a critical fit to the best available measurements of vibrational frequencies, supplemented by new, accurate (and correctly interpreted) data of this kind, might provide new sets of empirical potentials of superior quality in reproducing the values of thermodynamic functions, often within their experimental accuracy. Such calculations of thermodynamic functions for a certain mineral might use crystallographic data, or eventually might not in view of the rapid advances in crystal-structure modeling.

All possible experimental information is important for checking the validity of the vibrational model. In view of their actual physical meaning, experimental values of ADP obtained from accurate crystal-structure refinement can be particularly useful for comparison with corresponding theoretical estimates, because definite information about the vibrational behavior of every atom in the crystal can be obtained in the whole Brillouin zone.

In extending our calculations to complex silicates, we concentrated on beryl because of its considerable mineralogical and petrological interest. For this mineral, good (and pure) natural crystals are readily available, and there are several reliable experimental data sets for comparison. These data sets include accurate crystal-structure determinations (Morosin 1972; Hazen et al. 1986; Evdokimora et al. 1988; Artioli et al. 1993), Raman and infrared spectra (Gervais et al. 1972; Adams and Gardner 1974; Kurazhkovskaya and Plyusnina 1984; Kurazhkovskaya et al. 1987; Hofmeister et al. 1987; Hagemann et al. 1990), and thermodynamic functions (Barton 1986; Hemingway et al. 1986).

#### PROCEDURE OF CALCULATION

Our calculations follow the classic rigid-ion lattice-dynamical model (e.g., Pilati et al. 1990, 1996a, 1996b). The entropy for example is given by (see Equation 3 in Pilati et al. 1996b):

$$S(T, V, T) \approx S(T, V_{298}) + \alpha^2 V K_T (T - 298). \quad (1)$$

Equation 1 implies that  $\alpha$ ,  $V$ , and  $K_T$  (or at least their product) are independent of temperature. However, for beryl  $\alpha$  is strongly temperature dependent. Therefore, the linear equation  $\alpha = \alpha_0 + \beta_0 T$  was adopted, where  $\alpha_0$  (=

$-1.12 \times 10^{-6} \text{ K}^{-1}$ ) and  $\beta_0$  (=  $1.03 \times 10^{-8} \text{ K}^{-2}$ ) were derived by least-squares fits of Morosin's (1972) data. Since:

$$\begin{aligned} \partial(\alpha K_T)/\partial T &= K_T \partial\alpha/\partial T + \alpha \partial K_T/\partial T \\ &= \beta_0 K_T + (\alpha_0 + \beta_0 T) \partial K_T/\partial T \\ &= A_g + B_g T \end{aligned} \quad (2)$$

where

$$A_g = \beta_0 K_T + \alpha_0 \partial K_T/\partial T \quad \text{and} \quad B_g = \beta_0 \partial K_T/\partial T,$$

and:

$$(\partial C_V/\partial V)_T = T[\partial(\alpha K_T)/\partial T]_V \quad (3)$$

$$\begin{aligned} C_V - C_V(298) &= \int_{V_{298}}^V (TA_g + T^2 B_g) dV \\ &= (TA_g + T^2 B_g)(V - V_{298}) \end{aligned} \quad (4)$$

where  $C_V(298)$  is the specific heat at constant volume and at temperature  $T$ , calculated using the crystal structure data at 298 K. And since:

$$V - V_{298} \approx V_{298}[\alpha_0(T - 298) + \beta_0/2(T^2 - 298^2)] \quad (5)$$

it will become:

$$\begin{aligned} C_V - C_V(298) &= V_{298}[\alpha_0(T - 298) + \beta_0/2(T^2 - 298^2)] \\ &\quad \times (TA_g + T^2 B_g). \end{aligned} \quad (6)$$

Consequently, by knowing  $\alpha_0$ ,  $\beta_0$ , and the volume, it is possible to correct the lattice-dynamical estimate of the specific heat,  $C_V$ , at any temperature, using crystal-structure data at 298 K and Equation 6. In most cases (for instance with diopside), such a correction, which is clearly related to  $(\partial C_V/\partial V)_T$ , is small or negligible. However, for beryl,  $\alpha$  increases strongly with temperature. For this reason the above contribution becomes important and has been considered in deducing the values reported in Table 4; for instance, at 1800 K it amounts to +9.31 J/(mol·K). For maximum efficiency in applying these corrections, the value of the derivative  $\partial K_T/\partial T$  should also be known; unfortunately, no data of this kind are available for beryl. In performing our calculations, we assumed this derivative to be zero. However, if we instead assume it to be on the order of  $-0.02 \text{ GPa/K}$ , as observed for other silicates such as garnets (see Hofmeister and Chopelas 1991), then the above contribution would decrease to +7.46 J/(mol·K). All these figures give an idea of the importance of the various terms in such corrections and emphasize the need of a more complete set of measurements of unit-cell parameters at different temperatures and pressures.

The total correction to the entropy can be evaluated by using:

TABLE 1. Empirical potentials used in this paper

Atomic charge (e)			
	Si	Al	Be
	-1.46109	-1.40477	-1.18432
Stretching potentials*			
	A	B	C
Si-O	2618.68	0.769077	1.65009
Al-O	261.563	1.37922	1.91963
Be-O	6738.53	0.315366	1.69602
O-O (<5.5 Å)	9.19103	0.816777	3.60851
Bending potentials†			
	A	B	C
O-Si-O	-0.113204	-1.28218	0.747949
O-Al-O	0.447430	0.465711	-0.117495
O-Be-O	0.320159	0.248974	0.697252
Si-O-Si‡	0.309488		
Al-O-Al‡	7.33446E-02		
Be-O-Be‡	6.14341E-03		
Be-O-Si‡	-6.58876E-02		
Be-O-Al‡	-8.76495E-02		
Al-O-Si‡	0.213679		
Bending-stretching potentials§			
	A	B	C
O-Si-O/Si-O	-7.42877E-03	-4.33292E-02	109.47
O-Al-O/Al-O	0.159498	-2.01806E-03	90.00
O-Be-O/Be-O	0.150689	1.77607E-02	109.47
Stretching-stretching potentials (mdyn-Å)			
	Si-O/Si-O	Al-O/Al-O	Be-O/Be-O
	0.112083	3.93192E-03	-2.68119E-02

Notes: For coulombic interactions, the reciprocal lattice was sampled up to a limiting value of  $d^* = 1.7 \text{ \AA}^{-1}$ . The atomic charge of O was calculated by difference to satisfy charge balance.

\* Morse functions as: Energy (kJ/mol) =  $A[\exp(-2B(r - C)) - 2 \exp(-B(r - C))]$ , where  $r$  is the distance in Å.

†  $K$  (mdyn-Å/rad<sup>2</sup>) =  $A + B \cos\beta + C \cos^2\beta$ , where  $\beta$  is the bond angle.

‡  $K = 0.00$  if  $\beta > 150^\circ$ .

§  $K$  (mdyn-rad) =  $A + B(\beta - C)$ ,  $\beta$  in degrees.

$$\int_{V_{298}}^V [C_v - C_v(298)]/T dT$$

$$= V_{298} \int_{298}^T [\alpha_0(T - 298) + \beta_0/2(T^2 - 298^2)]$$

$$\times [A_g + TB_g] dT. \quad (7)$$

together with Equation 2 in Pilati et al. (1996b).

Finally, we think that some delicate points need additional comments. Our procedure differs from the usual, mainly because we start directly from the crystal structure at room temperature, and no attempt is made in relaxing it. This procedure can be justified by several reasons, besides saving computing time. For instance, in the harmonic approximation the frequencies are determined by the second derivatives of the potential energy with respect to the atomic positional parameters; therefore, if a potential is derived (as it is here) from fits to these frequencies only, no direct information concerning either the value of energy or its first derivatives can be deduced. Therefore, to obtain the first derivatives, which are necessary for energy minimization, appropriate integration constants should be assigned, so that for the series of substances studied the differences between all observed crystal structures and the corresponding energy-minimum models are the smallest possible. If the energy of formation of the

crystal is also needed, then a further series of integration constants would be necessary. This search for more complete potential functions on this basis is a topic of future work.

The a priori deduction of a crystal structure, i.e., the process of following theoretical procedures only, either employing quantum mechanics exclusively, or using empirical functions that are valid for a group of different substances, is an outstanding task, which has actually been achieved in recent times for a few minerals (for examples of applications of quantum mechanics to minerals, see Lasaga and Gibbs 1987 or Silvi et al. 1991). The task becomes formidable if performed on a free-energy minimization basis rather than on energy minimization. However, potential energy minimization provides one solution only (temperature independent), whereas free energy should be considered instead if temperature-dependent results are required. The simplest possible way to attain such goals is provided by quasi-harmonic lattice-dynamical calculations, and such notably long calculations were indeed performed in a few cases for organic crystals (Filippini and Gramaccioli 1981), and also for minerals (see, for instance: Price et al. 1987b; Patel et al. 1991; Catti et al. 1993), with interesting results. However, again we emphasize that the scope of our present work is different. It has been limited to deriving physical-chem-

TABLE 2. Vibrational spectra (cm<sup>-1</sup>) at room temperature

	Obs1	Obs2	Obs3	Calc
A <sub>2u</sub> (TO)	201		207	213
	361		368	404
	419	423	425–470	449
	532	537	538?	532
	734	733	743	759
	924	916		948
	975	978?		
		1054		
A <sub>2u</sub> (LO)	210			216
	376	375		416
	484	473		497
	554			537
	772	771		770
			1045	
E <sub>1u</sub> (TO)				189
	257		258	262
				312
	350	350	349	356
	381	382	381–387	377
				399
	500	488	482	505
	536	519?		531
		588	557	577
	600		590–602	602
	660	652	653	650
		674	668?	
		803	691	
			823	
				917
	962	955	960	
1020	1016	953	1046	
			1135	
1198		1185	1138	
		1279		
E <sub>1u</sub> (LO)				189
	262			263
				314
	350			358
	387			377
				407
	510	502		514
	564	560		542
			594	
E <sub>1u</sub> (LO)	660			611
	706	703		674
	828	825		939
	1002	995		971
	1032			1058
				1135
			1175	
E <sub>2g</sub>	146	138–144		140
	187	176–186		171
	291	288–294		297
	318	315–320		332
	397	396–398		340
	424	413–422		411
	444	441–443		504
	565	560–564		564
	583	571–582		599
	685	683–686		705
		727–748		736
	772	757–770		767
	914	907–916		933
	1005	1000–1006		950
		1018		
1225	1191–1229		1143	
1243	1215–1243		1147	
E <sub>1g</sub>	145	138–140		140
	131	146		154
	188	192		208
	254	247–254		234
	297	296–300		308

TABLE 2—Continued

	Obs1	Obs2	Obs3	Calc
	383	381–384		362
	450	439–449		468
	529	521–526		510
		536		529
		617		636
	683	675–686		
	770	768–770		
	918	918–919		939
				977
	1012	1007–1012		1039
A <sub>1g</sub>	214	240–242		249
	324	320–323		324
	396	394–399		442
	626	615–624		669
	686	682–685		717
	1068	1066–1068		981
	1125	1113–1139		1134

Note: Obs1 = single-crystal data from Adams and Gardner (1974); Obs2 = single-crystal Raman data from Hagemann et al. (1990); here the observed range is reported for a series of four different specimens examined by these authors; in the same column the IR data obtained by Gervais et al. (1972) are also reported; Obs3 = single-crystal IR data from Hofmeister (1987).

ical data from crystallographic information, whenever it is available; at the same time, we are testing the accuracy of estimates of thermodynamic functions that were derived on such grounds. If the free-energy minimum instead of the energy minimum is considered, then there is no sense in relaxing the crystal structure until it reaches a minimum of potential energy.

Other delicate points concern the dependence of the crystal structure on temperature. For instance, in the process of deducing temperature-dependent physical data (e.g., thermodynamic properties) for a certain phase one possibility might be to use a different crystal structure at each temperature. However, in spite of widespread beliefs, empirical potentials derived from best fits to a group of substances at one temperature (as they are here) might not give a comparable performance at different temperatures. This inconvenience may occur because, due to the effect of thermal motion, the experimental values of bond distances, as they are deduced from the differences in the final atomic coordinates after refinement of crystal structures, are not necessarily equal to the actual (time and space) averages of the distances between the corresponding atoms. Such a problem is the basis for the need to correct interatomic distances for thermal motion (e.g., Cruickshank 1956; Busing and Levy 1964; Schomaker and Trueblood 1968; Johnson 1970, 1980; Scherlinger 1972). Although the effects of bond-length correction might seem negligible for our purposes, they are not necessarily so, because most potentials are quite steep, and what often counts is the difference between comparatively large values. Therefore, in view of our testing a procedure until its limits of significance, even such a possibility should be taken into account, at least by roughly stating that for similar chemical units within a group of minerals at a certain temperature the corresponding ap-

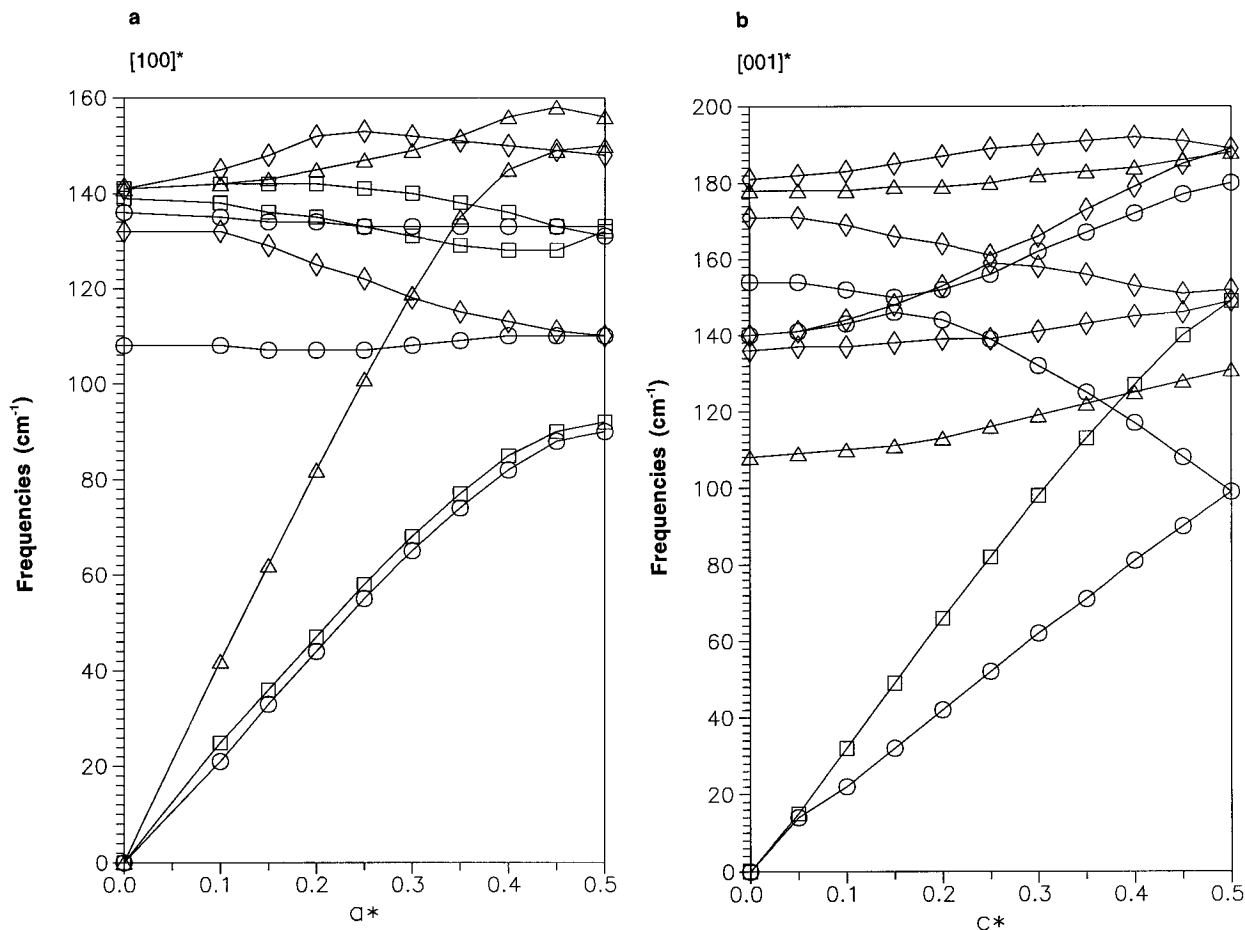


FIGURE 1. Lower branches of calculated phonon dispersion curves for beryl along  $[100]^*$  (a) and  $[001]^*$  (b). Different symbols refer to different symmetry representations ( $\Sigma_1$ - $\Sigma_4$  and  $\Delta_1$ - $\Delta_4$ , respectively).

parent bond distances (i.e., those uncorrected for thermal libration) are comparable. In any case, such bond distances are not the true ones to be considered for comparison with quantum-mechanical data, and there are also some reasons for doubting whether the extension of the procedure to the corresponding sets of atomic distances (uncorrected for thermal libration) taken at different temperatures is fully justified.

#### ANALYSIS OF RESULTS AND DISCUSSION

As in our previous work, all parameters of the force field used for beryl (including the atomic charge), and reported in Table 1, were obtained on a best-fit basis to the vibrational frequencies of quartz and silicates, such as members of the olivine group (forsterite, fayalite, tephroite, and monticellite), garnet (andradite), andalusite, diopside, beryl, and some oxides containing Al or Be, such as corundum, chrysoberyl, and bromellite. Most of these data are Raman- and infrared-active frequencies obtained by different authors (see Pilati et al. 1990, 1993a, 1993b, 1994, 1995, 1996a, 1996b). The lowest branches of the phonon dispersion curves were included when

available (quartz, forsterite, and andalusite). With respect to the corresponding force fields reported in our previous papers (see Pilati et al. 1996b) there are slight differences. Such variations can be accounted for mainly by the increased number of fitted data.

The calculated Raman- and infrared-active frequencies are reported in Table 2, together with the corresponding experimental results obtained by various authors. The agreement is very good, especially in the low-frequency range, and is in line with the expected performance of a rigid-ion model and with our weighting scheme in deriving the potential parameters. We also obtained the phonon dispersion curves shown in Figure 1, for comparison with future experimental determinations.

In view of the good agreement of our model with the available spectral data, the interpretation of the normal modes in the crystal is reasonably grounded, especially for the lowest frequencies. As it was shown for other silicates, including ring structures such as that of benitoite (e.g., Kim et al. 1993) each normal mode implies extensive deformation in the crystal. Such behavior can be easily explained, because here a single molecular group does

**TABLE 3.** Anisotropic displacement parameters ( $\times 10^4$ ) at room temperature (298 K) and isotropic or equivalent  $B_{\text{eq}}$ 

		Obs1	Calc1	Obs2	Obs3	Obs4	Obs5	Obs6	Calc2
Si	$U_{11}$	34(1)	35	26(6)	53(6)	41(2)	31(2)	51(17)	16
	$U_{22}$	30(1)	28	27(6)	43(6)	39(2)	27(2)	53(19)	14
	$U_{33}$	32(1)	39	31(8)	26(6)	42(2)	36(2)	44(10)	16
	$U_{12}$	16(1)	16	11(5)	34(5)	20(2)	15(1)	42(16)	8
	$B_{\text{eq}}$	0.25(1)	0.27	0.23(4)	0.29(4)	0.32(2)	0.24(2)	0.34(7)	0.12
Al	$U_{11}$	37(1)	36	30(10)	46(7)	46(2)	23(2)	50(19)	18
	$U_{33}$	39(1)	40	30(10)	30(10)	42(4)	34(3)	-3(19)	19
	$B_{\text{eq}}$	0.30(1)	0.30	0.27(7)	0.33(5)	0.35(2)	0.21(2)	0.26(9)	0.15
	$U_{11}$		87	61(5)	65(5)			40(14)	49
Be*	$U_{22}$		39	49(5)	53(6)			30(17)	25
	$U_{33}$		56	59(6)	53(7)			55(13)	33
	$U_{12}$		19	24(3)	26(3)			15(16)	13
	$B_{\text{eq}}$	0.47(1)	0.52	0.45(3)	0.46(3)	0.60(4)	0.45(2)	0.33(7)	0.30
	O1	$U_{11}$	101(5)	95	101(5)	113(5)	113(7)	103(5)	92(15)
$U_{22}$		71(1)	67	76(6)	80(5)	79(6)	75(5)	41(14)	31
$U_{33}$		117(1)	116	119(7)	163(6)	138(6)	128(6)	126(9)	47
$U_{12}$		66(1)	63	70(4)	78(4)	67(6)	72(5)	42(13)	27
$B_{\text{eq}}$		0.68(1)	0.65	0.69(4)	0.85(3)	0.87(5)	0.80(3)	0.65(6)	0.28
O2	$U_{11}$	71(1)	60	69(5)	109(4)	89(4)	73(3)	79(10)	30
	$U_{22}$	53(1)	45	50(5)	113(4)	65(4)	50(3)	100(9)	25
	$U_{33}$	53(1)	52	54(6)	70(4)	73(4)	60(3)	80(6)	25
	$U_{12}$	30(1)	22	29(3)	72(3)	38(3)	30(2)	64(9)	12
	$U_{13}$	23(1)	-16	-22(2)	-52(3)	-25(3)	-21(2)	-37(6)	-7
	$U_{23}$	5(1)	-1	-3(2)	-36(3)	-7(3)	-3(3)	-37(6)	-1
	$B_{\text{eq}}$	0.47(1)	0.42	0.46(3)	0.71(3)	0.62(3)	0.47(2)	0.62(4)	0.21

Notes: The temperature factor is in the form:  $T = \exp[-2\pi^2(U_{11}h^2a^{*2} + U_{22}k^2b^{*2} + U_{33}l^2c^{*2} + 2U_{12}hka^*b^* + 2U_{13}hla^*c^* + 2U_{23}klb^*c^*)]$ . Obs1 = X-ray diffraction data, from Morosin (1972); Obs2 from Artioli et al. (1993), aquamarine at 295 K, neutron diffraction data; Obs3 from Artioli et al. (1993), morganite at 295 K, neutron data; Obs4 from Artioli et al. (1993), morganite at 295 K, X-ray data; Obs5 from Artioli et al. (1993), aquamarine at 295 K, X-ray data; Obs6 from Artioli et al. (1993), morganite at 30 K, neutron data; Calc1 our calculations for  $T = 298$  K; Calc2 our calculations for  $T = 30$  K. For each value shown in this table, the standard deviation follows in parentheses.  $U$  refers to the specific atoms whose coordinates are reported in the papers mentioned (which are the same for all the papers).

\* X-ray data with isotropic ADP.

not exist; all atoms and their coordination polyhedra are strictly connected to each other.

On considering the observed spectral data in some detail, the Raman-active modes ( $E_{1g}$ ,  $E_{2g}$ ,  $A_{1g}$ ) can be seen to agree very well with our calculations. The few cases showing some disagreement are probably spurious. For instance, the  $A_{1g}$  mode observed by Adams and Gardner (1974) at  $214 \text{ cm}^{-1}$  is too low with respect to our calculations; however, Hagemann et al. (1990) obtained for the same mode a range of values in quite good agreement with our results. Similarly, an  $E_{2g}$  mode calculated by us at  $736 \text{ cm}^{-1}$ , and two  $E_{1g}$  modes calculated at  $529$  and  $636 \text{ cm}^{-1}$ , respectively, which do not match any data reported by Adams and Gardner, are instead in good agreement with the Hagemann et al. measurements. There are, however, a few frequencies reported by all the experimental authors that do not show comparable agreement with our model. For instance the  $A_{1g}$  frequency reported around  $396 \text{ cm}^{-1}$  and one  $E_{2g}$  frequency observed in the range  $300\text{--}450 \text{ cm}^{-1}$  instead might be combination bands or overtones, whereas an  $E_{2g}$  frequency around  $500 \text{ cm}^{-1}$  might be expected.

On the whole, the agreement of the IR-active modes with the measured spectra is not as good as for the Raman-active modes, probably owing to experimental difficulties. In any case, in agreement with Adams and Gardner (1974), the observed  $A_{2u}(\text{TO})$  frequencies higher than  $950 \text{ cm}^{-1}$  should not be fundamentals. A low  $E_{1u}$  frequency (around  $190 \text{ cm}^{-1}$ ) as well as another one around

$310 \text{ cm}^{-1}$  are predicted by our model, whereas the very high one ( $1279 \text{ cm}^{-1}$ ) observed by Hofmeister et al. (1987) should not be a fundamental, in agreement with either Adams and Gardner (1974) and Gervais et al. (1972). An  $E_{1u}$  frequency of about  $580 \text{ cm}^{-1}$  that is predicted by our model and does not match Adams and Gardner's (1974) data, is however in good agreement with the other experimental authors; whereas a series of frequencies in the range  $700\text{--}800 \text{ cm}^{-1}$ , which do not match our calculations, were not observed by Adams and Gardner (1974).

Anisotropic atomic displacement parameters, calculated for all the independent atoms in the crystal structure, are reported in Table 3. For comparison, in the same table a selection of corresponding experimental data obtained from some accurate crystal structure refinements are reported. The first set of such data, labeled Obs1, is from Morosin (1972), in connection with a detailed study of both the crystal structure and thermal expansion of the mineral. In a more recent work, Artioli et al. (1993) published data for two varieties of beryl, morganite and aquamarine, obtained by both X-ray and neutron diffraction (labeled Obs2–Obs5). A set of neutron data at low temperature (30 K: Obs6) is also reported by Artioli et al. (1993) for morganite; however, the accuracy of this data set is low (see below).

On examining Table 3, there is remarkable agreement of our calculations with the corresponding experimental data. Such agreement is especially evident for Morosin's

**TABLE 4.** Values of the specific heat and entropy (J/mol-K) at various temperatures

$T$ (K)	$C_p$ obs	$C_p$ calc	$C_v$ calc	$S$ obs	$S$ calc (corrected)	$S$ calc (uncorrected)
15	2.09	0.41	0.41	0.90	0.12	0.12
30	9.32	5.72	5.72	4.11	1.52	1.52
60	51.57	45.34	45.34	21.61	15.90	15.90
90	110.0	101.04	101.04	53.32	44.61	44.61
120	169.9	158.98	158.98	93.18	81.64	81.64
150	227.4	214.58	214.58	137.4	123.2	123.2
180	280.1	265.97	265.97	183.5	166.9	166.9
210	328.0	312.67	312.67	230.4	211.5	211.5
240	371.0	354.75	354.73	277.1	256.0	256.0
270	409.1	392.41	392.39	323.0	300.0	300.0
298	417.8	423.86	423.82	346.7( $\pm 4.7$ )	340.3	340.3
400	508.6	512.59	512.43	483.1	478.4	478.4
500	568.1	570.32	569.63	603.4	599.4	599.3
600	609.1	608.67	607.91	710.8	707.0	706.8
700	638.3	635.49	634.19	807.0	802.9	802.6
800	659.8	654.82	652.77	893.7	889.2	888.6
900	676.3	669.32	666.28	972.5	967.1	966.3
1000	689.6	680.67	676.36	1044	1038	1037
1100	700.9	689.94	684.06	1111	1104	1102
1200	711.0	697.07	690.06	1172	1164	1162
1300	720.7	704.91	694.81	1229	1220	1217
1400	730.5	711.43	698.63	1283	1273	1269
1500	740.7	717.72	701.76	1334	1322	1317
1600	751.7	723.93	704.34	1382	1369	1363
1700	763.6	730.24	706.50	1428	1412	1405
1800	776.7	736.76	708.32	1472	1455	1446

Notes: Observed values of thermodynamic functions from Hemingway et al. (1986). Below 298 K, the only available data (reported here) are for a hydrated phase,  $\text{Be}_3\text{Al}_2\text{Si}_6\text{O}_{18} \cdot 0.36\text{H}_2\text{O}$ ; according to these authors, at room temperature (298.15 K) the difference in  $C_p$  between the hydrated phase and anhydrous beryl is 23.6 J/mol-K, and the difference in  $S$  is 18.5 J/mol-K. The values for  $C_p$  calculated by us were obtained by adding the  $C_p - C_v = \alpha^2 VTK_T$  difference to the corresponding calculated value of  $C_v$  (here evaluated using Eq. 9). For this purpose, the average value of the volume expansion coefficient  $\alpha = (-1.126 + 0.01037) \times 10^{-6} \text{ K}^{-1}$  from 298–1100 K was taken from least-squares interpolation of Morosin's (1972) unit-cell data. Below 298 K, in lack of experimental data, as a rough approximation, a linear interpolation down to a zero value at 0 K was assumed. For the bulk modulus the value  $K_T = 170 \text{ GPa}$  found by Hazen et al. (1986) was used. The values of entropy calculated by us and reported in column 6 were corrected for anharmonicity (thermal expansion) using Equation 10 and the data mentioned above.

data, which are the most accurate. On these grounds, there is even reason for believing that in Morosin's reported value of  $U_{13}$  for O2 a minus sign is missing, because we have only notable disagreement. On the other hand, all the other measured values have a minus sign.

For all silicates and oxides we have examined so far (for a more detailed discussion see Pilati et al. 1996b), our calculations show that the zero-point contribution is remarkably large (nearly 50% of the room-temperature value and practically coinciding with the calculated results at  $T = 30 \text{ K}$ ). The low-temperature neutron-diffraction data reported for morganite by Artioli et al. (1993) would be quite useful for providing a further experimental confirmation of such a phenomenon; however, the accuracy of the ADP obtained in such a refinement is too low for adequate comparison with our theoretical data (for instance, the measured values of the ADP at 30 K are sometimes higher than the corresponding values at room temperature), and in any case the main scope of the work of Artioli et al. was that of locating  $\text{H}_2\text{O}$  molecules and the alkali cations in the beryl structure.

Calculated values of thermodynamic functions, such as the specific heat  $C_p$  and entropy  $S$  at different temperatures, according to our model and procedure are shown in Table 4; they are compared with the corresponding experimental values reported by Hemingway et al. (1986, Tables 5 and 16). At 298 K and above, the agreement is

remarkably good; for instance at room temperature (298 K) the disagreement for  $C_p$  and  $S$  with the corresponding experimental data is 1.5 and 1.8%, respectively, and the situation remains quite satisfactory up to 1000 K and above. In particular, for entropy, at room temperature the difference with respect to the result of our lattice-dynamical calculations is almost equal to the uncertainty [ $\pm 4.7 \text{ J}/(\text{mol}\cdot\text{K})$ ] of the corresponding experimental value, as given by Barton (1986). At very high temperature, the calculated values are systematically lower than the corresponding experimental data. This phenomenon might be linked to inadequacy of the harmonic model.

At low temperature ( $\leq 298 \text{ K}$ ) the presence of  $\text{H}_2\text{O}$  in most beryl specimens has caused some concern in establishing the thermodynamic properties of this mineral. Below 298 K, the data reported by Hemingway et al. (1986) relates to the hydrated phase only, and no data relative to the anhydrous phase have ever been reported. The notable difference between observed and calculated values of thermodynamic functions at low temperature can be explained on such a basis. Another source of uncertainty is caused by the lack of data, such as the coefficients of thermal expansion in the range 0–273 K, that are necessary to correct our lattice-dynamical results (see above). In the present work, these coefficients have been estimated as a linear interpolation from zero (at 0 K, in agreement with the third law) to the experimental value

at 273 K, the lowest temperature at which the unit-cell data have been measured.

The room-temperature value for the entropy of the anhydrous phase [ $346.7 \pm 4.7$  J/(mol·K)] was obtained by Barton (1986) from multiple regression analysis. To account for the entropy difference between hydrated beryl (for which a series of heat-capacity measurements from 0 to 298 K is available) and the anhydrous phase, Hemingway et al. (1986) assumed the entropy of H<sub>2</sub>O in beryl to be 55 J/(mol·K) at 298 K, because of its similarity in bonding to some zeolites (analcime, clinoptilolite); under this assumption a value of  $345 \pm 5$  J/(mol·K) for the entropy of anhydrous beryl at 298 K was derived, a figure that is closer to our own lattice-dynamical results. The excellent agreement between all these different models and estimates supports the validity of such procedures.

For low temperatures, such as 30 K and below, Hemingway et al. (1986) remarked that the heat capacity of beryl is unexpectedly high for a compound with such a low mean atomic weight. According to their own calculations, on the basis of a Debye model, these authors estimated a heat capacity for beryl at 16 K that is only about 19% of the observed value. On looking at Table 4, we also notice a similar disagreement at 15 K, using our Born-von Karman model, leading to a corresponding disagreement for entropy. Such disagreement could be attributed to the presence of absorbed H<sub>2</sub>O, but Hemingway et al. (1986) noticed that the heat capacity of the amount of ice present (0.36 mol) is also only 20% of the measured heat capacity at 16 K, and on this basis this difference remains unexplained. In our case, however, a comparison with ice might not be appropriate, in view of the statistical disorder of this substance, a disorder that (hopefully) could not exist for trapped H<sub>2</sub>O molecules in the channels of the beryl structure, owing to the impossibility of having the same set of hydrogen bonds.

Apart from these minor problems, in general our application of empirical potentials and harmonic lattice-dynamics to beryl confirms the possibility of deriving several properties, crystallographic or non-crystallographic by using a routine procedure and widely transferable potentials.

#### ACKNOWLEDGMENTS

Financial contributions from CNR and MURST are gratefully acknowledged. Valuable help from Luigi Saibene and Italo Camprostrini concerning the graphics is also acknowledged.

#### REFERENCES CITED

- Adams, D.M. and Gardner, I.R. (1974) Single-crystal vibrational spectra of beryl and diopside. *Journal of the Chemical Society, Dalton*, 1502–1505.
- Artoli, G., Rinaldi, R., Ståhl, K., and Zanazzi, P.F. (1993) Structure refinements of beryl by single-crystal neutron and X-ray diffraction. *American Mineralogist*, 78, 762–768.
- Barton, M.D. (1986) Phase equilibria and thermodynamic properties of minerals in the BeO-Al<sub>2</sub>O<sub>3</sub>-SiO<sub>2</sub>-H<sub>2</sub>O (BASH) system, with petrologic applications. *American Mineralogist*, 71, 277–300.
- Busing, W. and Levy, H.A. (1964) The effect of thermal motion on the estimates of bond length from diffraction measurements. *Acta Crystallographica*, 17, 142–146.
- Catti, M., Pavese, A., and Price, G.D. (1993) Thermodynamic properties of CaCO<sub>3</sub> calcite and aragonite: a quasi-harmonic calculation. *Physics and Chemistry of Minerals*, 19, 472–479.
- Cruickshank, D.W.J. (1956) Errors in bond lengths due to rotational oscillation of molecules. *Acta Crystallographica*, 9, 757–758.
- Dove, M.T., Winkler, B., Leslie, M., Harris, M.J., and Salje, E.K.H. (1992) A new interatomic potential model for calcite: Applications to lattice dynamics studies, phase transition, and isotope fractionation. *American Mineralogist*, 77, 244–250.
- Evdokimova, O.A., Belskoneva, E.L., Tsirelson, V.G., and Urusov, V.S. (1988) Accurate X-ray investigation of the structure, the electron density and the electrostatic potential distribution in beryl. *Geokhimiya*, 1988, 677–687.
- Filippini, G. and Gramaccioli, C.M. (1981) Deriving the equilibrium conformation in molecular crystals by the quasi-harmonic procedure: some critical remarks. *Acta Crystallographica*, A37, 335–342.
- Gervais, F., Piriou, B., and Cabannes, F. (1972) Anharmonicity of infrared vibration modes in beryl. *Physica Status Solidi*, B51, 701–712.
- Ghose, S., Choudhury, N., Chaplot, S.L., Pal Chowdury, C., and Sharma, S.K. (1994) Lattice dynamics and Raman spectroscopy of protoenstatite Mg<sub>2</sub>Si<sub>2</sub>O<sub>6</sub>. *Physics and Chemistry of Minerals*, 20, 469–477.
- Gramaccioli, C.M. (1987) Spectroscopy of molecular crystals and crystallographic implications. *International Reviews in Physical Chemistry*, 6, 337–349.
- Hagemann, H., Lucken, A., Bill, H., Gysler-Sanz, J., and Stalder, H.A. (1990) Polarized Raman spectra of beryl and bazzite. *Physics and Chemistry of Minerals*, 17, 395–401.
- Hazen, R.M., Au, A.Y., and Finger, L.W. (1986) High-pressure crystal chemistry of beryl (Be<sub>3</sub>Al<sub>2</sub>Si<sub>4</sub>O<sub>18</sub>) and euclase, (BeAlSiO<sub>4</sub>OH). *American Mineralogist*, 71, 977–984.
- Hemingway, B.S., Barton, M.D., Robie, R.A., and Haselton, H.T., Jr. (1986) Heat capacities and thermodynamic functions for beryl, Be<sub>3</sub>Al<sub>2</sub>Si<sub>4</sub>O<sub>18</sub>, phenakite, Be<sub>2</sub>SiO<sub>5</sub>, euclase, BeAlSiO<sub>4</sub>(OH), bertrandite, Be<sub>2</sub>Si<sub>2</sub>O<sub>7</sub>(OH)<sub>2</sub>, and chrysoberyl, BeAl<sub>2</sub>O<sub>3</sub>. *American Mineralogist*, 71, 557–568.
- Hofmeister, A.M. and Chopelas, A. (1991) Thermodynamic properties of pyrope and grossular from vibrational spectroscopy. *American Mineralogist*, 76, 880–891.
- Hofmeister, A.M., Hoering, T.C., and Virgo, D. (1987) Vibrational spectroscopy of beryllium aluminosilicates: Heat capacity calculations from band assignments. *Physics and Chemistry of Minerals*, 14, 205–224.
- Johnson, C.K. (1970) An introduction to thermal motion analysis. In *FR. Ahmed, Ed., Crystallographic Computing*, p. 220–226. Munksgaard, Copenhagen, Denmark.
- (1980) Thermal motion analysis. In R. Diamond, S. Ramaseshan, and K. Venkatesan, Eds., *Computing in Crystallography*, p. 14.01–14.19. Indian Academy of Sciences, Bangalore, India.
- Keskar, N.R. and Chelikowsky, J.R. (1995) Calculated thermodynamic properties of silica polymorphs. *Physics of Chemistry and Minerals*, 22, 233–240.
- Kieffer, S.W. (1979a) Thermodynamics and lattice vibrations of minerals: 1. Mineral heat capacities and their relationships to simple lattice vibrational models. *Review of Geophysics and Space Physics*, 17, 1–19.
- (1979b) Thermodynamics and lattice vibrations of minerals: 2. Vibrational characteristics of silicates. *Review of Geophysics and Space Physics*, 17, 20–34.
- (1979c) Thermodynamics and lattice vibrations of minerals: 3. Lattice dynamics and an approximation for minerals with application to simple substances and framework silicates. *Review of Geophysics and Space Physics*, 17, 35–58.
- (1980) Thermodynamics and lattice vibrations of minerals: 4. Application to chain and sheet silicates and orthosilicates. *Review of Geophysics and Space Physics*, 18, 862–886.
- (1982) Thermodynamics and lattice vibrations of minerals: 5. Applications to phase equilibria, isotope fractionation and high-pressure thermodynamic properties. *Review of Geophysics and Space Physics*, 20, 827–849.
- Kihara, K. (1993) Lattice dynamical calculations of anisotropic tempera-



- ture factors of atoms in quartz, and the structure of  $\beta$ -quartz. *Physics and Chemistry of Minerals*, 19, 492–501.
- Kim, C.C., Bell, M.I., and McKeown, D.A. (1993) Vibrational analysis of benitoite ( $\text{BaTiSi}_3\text{O}_9$ ) and the  $\text{Si}_3\text{O}$  ring. *Physical Review*, B47, 7689–7877.
- Kurazhkovskaya, V.S. and Plyusnina, I.I. (1984) Infrared spectroscopic study of isomorphic substitutions in beryls. *Vestnik Moskovskogo Universitety, Seriya 4 Geologiya*, 39(3), 46–52.
- Kurazhkovskaya, V.S., Kupryanova, I.I., and Novikova, M.I. (1987) IR spectra of different crystal chemical types of beryl. *Novy Dannye Mineralov*, 34, 86–101.
- Lasaga, A.C. and Gibbs, G.V. (1987) Applications of the quantum mechanical potential surfaces to mineral physics calculations. *Physics and Chemistry of Minerals*, 14, 101–117.
- Morosin, B. (1972) Structure and thermal expansion of beryl. *Acta Crystallographica*, B28, 1899–1903.
- Patel, A., Price, G.D., and Mendelssohn, M.J. (1991) A computer simulation approach to modeling the structure, thermodynamics and oxygen isotope equilibria of silicates. *Physics and Chemistry of Minerals*, 17, 690–699.
- Pilati, T., Bianchi, R., and Gramaccioli, C.M. (1990) Lattice-dynamical estimation of atomic thermal parameters for silicates: forsterite  $\alpha\text{-Mg}_2\text{SiO}_4$ . *Acta Crystallographica*, B46, 301–311.
- Pilati, T., Demartin, F., Cariati, F., Bruni, S., and Gramaccioli, M. (1993a) Atomic thermal parameters and thermodynamic functions for chrysoberyl ( $\text{BeAl}_2\text{O}_4$ ) from vibrational spectra and transfer of empirical force fields. *Acta Crystallographica*, B49, 216–222.
- Pilati, T., Demartin, F., and Gramaccioli, C.M. (1993b) Atomic thermal parameters and thermodynamic functions for corundum ( $\alpha\text{-Al}_2\text{O}_3$ ) and bromellite ( $\text{BeO}$ ): a lattice-dynamical estimate. *Acta Crystallographica*, A49, 473–480.
- (1994) Thermal parameters for  $\alpha$ -quartz: a lattice-dynamical calculation. *Acta Crystallographica*, B50, 544–549.
- (1995) Thermal parameters for minerals of the olivine group: their implication on vibrational spectra, thermodynamic functions and transferable force fields. *Acta Crystallographica*, B51, 721–733.
- (1996a) Atomic displacement parameters for garnets: A lattice-dynamical evaluation. *Acta Crystallographica*, B52, 239–250.
- (1996b) Lattice-dynamical evaluation of atomic displacement parameters of minerals and its implications: The example of diopside. *American Mineralogist*, 81, 811–821.
- (1997) Transferability of empirical force fields in silicates: Lattice-dynamical evaluation of atomic displacement parameters and thermodynamic properties for the  $\text{Al}_2\text{OSiO}_4$  polymorphs. *Acta Crystallographica*, B53, 82–94.
- Price, G.D., Parker, S.C., and Leslie, M. (1987a) The lattice dynamics of forsterite. *Mineralogical Magazine*, 51, 157–170.
- (1987b) The lattice dynamics and thermodynamics of the  $\text{Mg}_2\text{SiO}_4$  polymorphs. *Physics and Chemistry of Minerals*, 15, 181–190.
- Rao, K.R., Chaplot, S.L., Choudhury, L., Ghose, S., Hastings, J.M., and Corliss, L.M. (1988) Lattice dynamics and inelastic neutron scattering from forsterite,  $\text{Mg}_2\text{SiO}_4$ : Phonon dispersion relation, density of states and specific heat. *Physics and Chemistry of Minerals*, 16, 83–97.
- Scheringer, C. (1972) A lattice-dynamical treatment of the thermal motion bond length correction. *Acta Crystallographica*, A28, 616–619.
- Schomaker, V. and Trueblood, K.N. (1968) On the rigid-body motion of molecules in crystals. *Acta Crystallographica*, B24, 63–76.
- Silvi, B., D'Arco, P., Saunders, V.R., and Dovesi, R. (1991) Periodic Hartree-Fock study of minerals: Tetracoordinated silica polymorphs. *Physics and Chemistry of Minerals*, 17, 674–680.
- Winkler, B., Dove, M.T., and Leslie, M. (1991) Static lattice energy minimization and lattice dynamics calculations on aluminosilicate minerals. *American Mineralogist*, 76, 313–331.

MANUSCRIPT RECEIVED AUGUST 1, 1996

MANUSCRIPT ACCEPTED JULY 14, 1997